

The global EVN view of the radio counterpart of GW170817

G. Ghirlanda*

INAF - Osservatorio Astronomico di Brera, Via E. Bianchi 28, I-23807 Merate (LC)

E-mail: giancarlo.ghirlanda@inaf.it

The detection of gravitational waves from the merger of two neutrons stars and, soon after, the discovery of its electromagnetic emission, GRB170817, confirmed that binary neutron star (BNS) mergers can be the progenitors of short Gamma Ray Burst (sGRB). This discovery probed that the bright optical–NIR thermal transient (the kilonova) is produced by the radioactively heated ejecta launched before and during the merger. Intriguingly, this event posed the question if, as expected in GRBs, a jet successfully broke out of the BNS ejecta or a more isotropic outflow is responsible for the non–thermal emission (from the X–ray to the radio band) observed for nearly one year post merger. Modelling the evolution of the lightcurve is insufficient to tell these two scenarios apart. High resolution global VLBI radio imaging (project GG084) show that the size of the source at 207.4 days is smaller than what expected in the case of a cocoon and is consistent with a narrow structured jet. This result implies that at least 10% of BNS should produce a successful jet.

*14th European VLBI Network Symposium & Users Meeting (EVN 2018)
8-11 October 2018
Granada, Spain*

*Speaker.

1. Introduction

The detection of gravitational wave (GW) signals from the inspiral and merger of binary black holes (BBH - [1]) and the detection of the GW signal produced by the merger of two neutron stars (BNS) accompanied by electromagnetic (EM) emissions (GRB170817 - [2]) sign the start of the era of multi-messenger astronomy.

GW/GRB170817 is characterized by three EM components which developed on different timescales:

1. ~ 2 seconds after the GW signal a dim (flux $\sim 2 \times 10^{-7}$ erg cm $^{-2}$ s $^{-1}$), relatively soft (peak of the νF_ν spectrum ~ 158 keV 1) and short (~ 2 s) burst of γ -ray photons was discovered by the Gamma Burst Monitor (GBM) on board Fermi ([3], also confirmed by INTEGRAL - [5]). At the source distance of 40 Mpc, GRB170817 had an isotropic equivalent luminosity of 10^{47} erg s $^{-1}$, i.e. three orders of magnitudes below the lowest luminosity ever measured in Short GRBs (e.g. [6]);
2. ~ 11 hours after the GW signal the bright (peak brightness $M_r \sim -15.8$) optical-NIR thermal emission (i.e. the kilonova (KN) SSS17a or AT2017gfo) was discovered [8, 7] and followed (e.g. [9]). The source showed a blue-to-red color evolution and was detected up to ~ 25 days.
3. ~ 10 days after the GW signal a slowly rising ($\propto t^{0.8}$ - [10]) non-thermal emission component (the afterglow, hereafter) was discovered in the X-ray and radio band [14, 13, 15]. This emission peaked, almost simultaneously at all observed frequencies, at ~ 150 days [16, 14] and eventually started fading rapidly.

The γ -rays probe that short GRBs can be produced by the merger of two neutron stars. The bright thermal emission is the first clear detection of a Kilonova: its emission is produced by the heating of the merger ejecta by radioactive decay of the r-process heavy elements produced in the merger ejecta (e.g. [17, 18]). The under-luminous short GRB 170817 suggests that either the merger produced an isotropic mildly relativistic outflow [19] or a relativistic jet seen largely off axis [9]. These two hypothesis predict a late time rise of the afterglow emission, produced by the deceleration of the nearly isotropic, mildly relativistic, fireball or of the off-axis jet, in agreement with the upper limits on the non-thermal emission until ~ 10 days post burst.

The discovery of the radio counterpart [20, 21, 22] and its subsequent monitoring [10, 14, 15] revealed a shallow increase of the flux, hardly explainable within the standard models. Proposed alternatives include a radial stratification of the velocity/energy of the nearly isotropic outflow (so called "cocoon" - [23, 11, 24]) or an angular distribution of the jet energy and bulk Lorentz factor (so called "structured jet" - [25, 26]). In the former case, slower shells deposit their larger energy in the forward shock thus producing a slowly rising flux. In the latter case, instead, the observed light curve is produced by the progressive deceleration of parts of the jet closer to its axis. The peak of the light curve at ~ 150 days corresponds to the tail of the outflow velocity distribution or to the core of the jet becoming visible by the off-axis observer.

¹The presence of a possible thermal tail has also been discussed - [3, 4]

In Fig. 1 the complete data set corresponding to different sampled frequencies (as shown in the legend) is reported. The two competing models, a structured jet (solid line) or a cocoon (dashed line) reasonably well account for the observed multi-wavelength data set. The parameters of these two models [27] are in agreement with those reported by other authors and with theoretical expectations. If the light curve modelling does not allow us to tell apart these two scenarios what other observations could?

For such a close source, the geometry of the outflow producing the non-thermal radiation could be probed by polarization measurements and imaging. The structured jet should have a larger displacement (when observed at two well separated epochs), a smaller size and larger polarization with respect to a more isotropic outflow (e.g. [28, 29]).

An upper limit of 12% on the linear polarization at 2.8 GHz measured 240 days after the merger was reported by [30]. However, while this seems to be consistent with the cocoon scenario, the possible presence of a component of the magnetic field non-parallel to the shock front can strongly reduce the polarization level also for a highly asymmetric configuration like that of a jet [28, ?].

Radio imaging of the source at 75 and 230 days with the High Sensitivity Array (HSA) revealed a significant displacement of ~ 2.67 mas in right ascension [12] which is compatible with the motion of the emission centroid of a relativistic jet pointing 20 degrees off the line of sight.

An independent probe of the jetted nature of the outflow is provided by high resolution radio imaging [27].

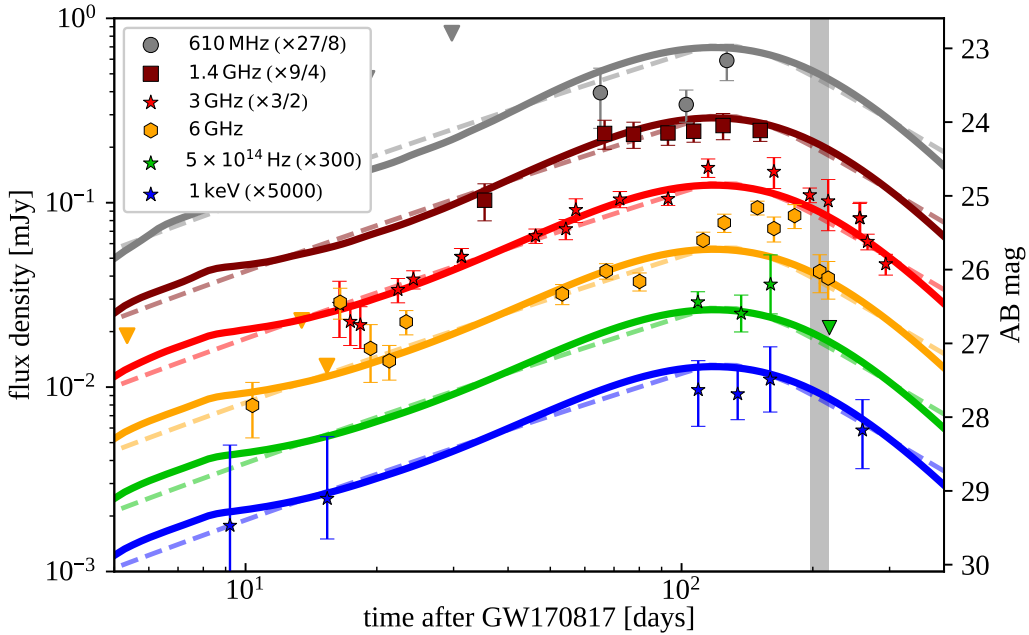


Figure 1: Multi-frequency light curve of the afterglow emission of GRB170817 (light curves corresponding to different frequencies are scaled as reported in the legend). Upper limits are shown by downward triangles. Model light curves for a structured jet (of 3.4° core aperture seen at 15° - solid line) and for a cocoon model with opening angle of 30° (dashed line) are shown. From [27].

2. Global-VLBI observations and results

We obtained a global VLBI observation (under the project code GG084) on 12-13 March 2018, corresponding to 204.7 days after the detection of the GW/EM 170817 event. This epoch corresponds to the peak phase of the multiwavelength light curve (shaded vertical grey stripe in Fig. 1). Radio observations were performed at a central frequency of 4.84 GHz and with a total bandwidth of 256 MHz. In the radio image, shown in the top panel of Fig.2, we detect the source with a peak brightness of $42 \pm 8 \mu\text{Jy}/\text{beam}$ which is consistent with the flux density of $47 \pm 7 \mu\text{Jy}$ obtained by interpolating the closest VLA observations [10] and with the 3σ upper limit of $60 \mu\text{Jy}/\text{beam}$ obtained by our supporting e-MERLIN quasi-contemporaneous campaign (project code CY6213). The source position is within the astrometrically corrected HST error circle and within 0.5 mas from the position recorded with the April 2018 HSA observation [10]. In particular our position at 204.7 days, which corresponds to an intermediate epoch between the two HSA ones (at 75 and 230 days - [10]), is consistent with the proper motion claimed by [10]. This is also shown in the top right zoom of the top panel of Fig.2.

As a first comparison of our two scenarios with the real image we proceeded as follows. We compute the surface brightness distribution of the two models and follow their evolution from the GW signal. This provides us with two maps (black images in Fig.2). These show the image size and surface brightness distribution expected if we have a structured jet seen at 15 degrees off axis (top left black image) or a cocoon model (top right black image). The latter model is conservatively assumed to have a quite large degree of asymmetry with an opening angle of 30 degrees (seen along its border). We derived the structured jet parameters by a MonteCarlo Markov Chain fit of (a) the centroid displacement of our observation with respect to the two HSA epochs and (b) the 3GHz light curve (red stars in Fig. 1). We then convolved (within AIPS) the theoretical images with the synthesized beam of our observation and added a noise map (with rms of $8 \mu\text{Jy}/\text{beam}$). The resulting images are shown in the bottom panels of Fig. 2 for the structured jet (left) and for the asymmetric cocoon (right). The same color coding for the flux density is used in all the images (the real and the theoretical ones). The comparison of the model images with the real one in Fig.2 clearly shows that the structured jet produces an image (left panel of Fig.2) that is strikingly similar to the real one (central panel of Fig.2). Instead a cocoon model, even allowing for a considerable degree of asymmetry, should have been resolved with the resolution of our observation and be undetected given the map rms (bottom right panel of Fig.2).

The relatively large rms of $8 \mu\text{Jy}/\text{beam}$ of our image (also due to the low elevation of the source and to the lack of VLA observations due to disk issues) hampers the estimate of the source size. Indeed, the standard approach, consisting in fitting the naturally weighted un-tapered image with a circular Gaussian, provides a size of 2.9 mas, i.e. comparable to the synthesized beam size (3.5×1.5 mas), but overestimates the flux density (i.e. 93μ) and violates the upper limit obtained with the e-MERLIN observation. A constrained fit, i.e. fixing the total source flux, yields a size of 1.3 ± 0.6 mas. In order to overcome the difficulties related to the low rms, we implemented a Bayesian method to estimate the source size which exploits all the information we have: (a) the source peak brightness measured from our un-tapered, naturally weighted, map of $42 \pm 8 \mu\text{Jy}/\text{beam}$, (b) a total flux density, as measured from the light curve by interpolating the two closest VLA detections, of $47 \pm 9 \mu\text{Jy}$. The aim of this procedure is to evaluate the posterior probability of the source

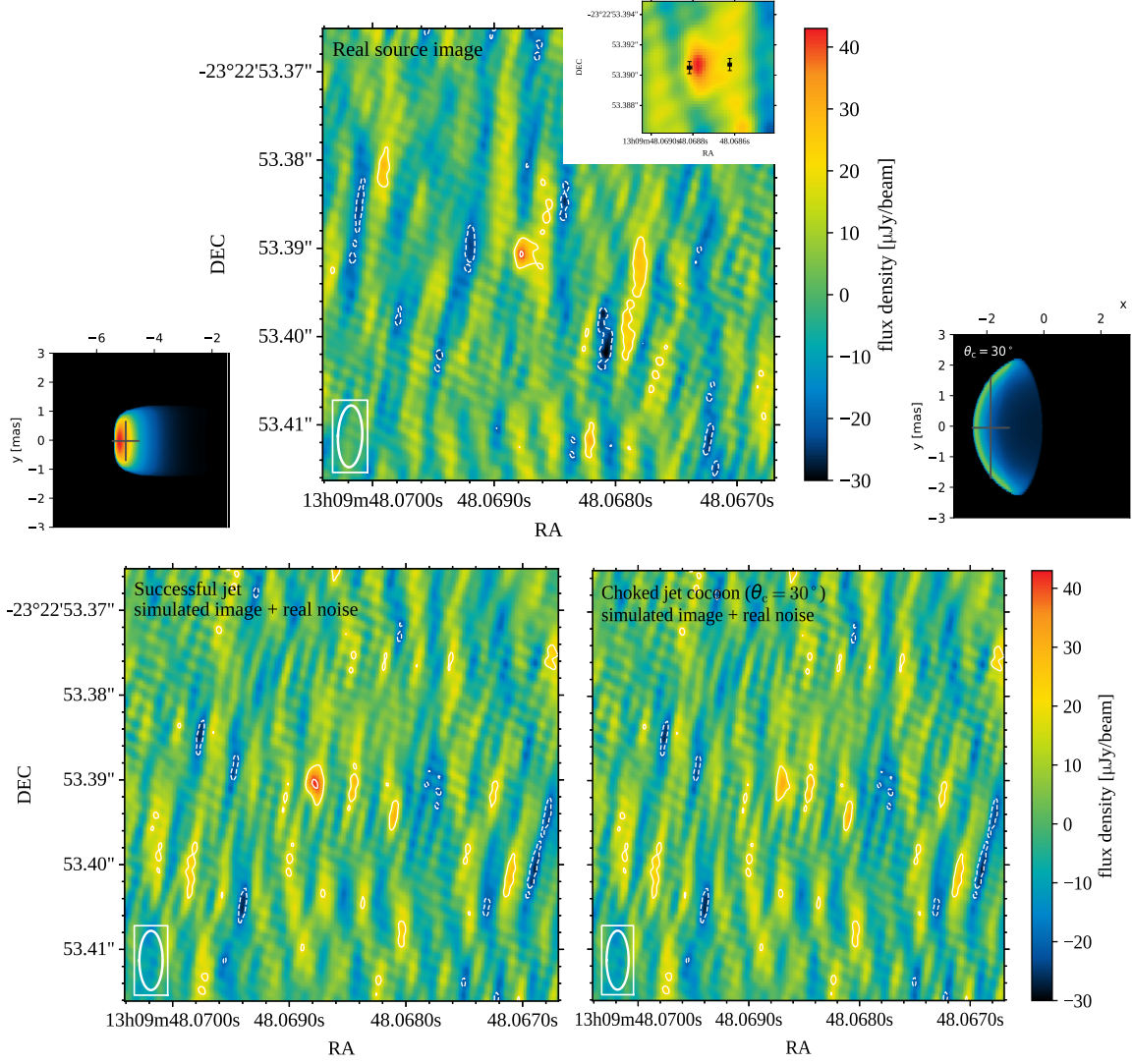


Figure 2: Top central panel: 5GHz image of the Global VLBI observation of GRB170817 performed 12-13 March 2018 (204.7 days after the burst/GW detection). The top right zoom shows the position of the two HSA observations (from Mooley et al. 2018) which bracket our detection. Bottom panels: synthetic images obtained by convolving the model images (for the structured jet and for the cocoon, right and left panels respectively) with the beam (shown in all images in the bottom left corner) and by adding a random noise as that measured in the true image. Adapted from [27].

size (either considering a circular Gaussian or a bi-dimensional one) given our peak brightness measurement (a) and assuming a flat prior on the total flux (b). This procedure, implemented through a MonteCarlo method, creates synthetic images (i.e. convolved with the beam size and added to a realization of the real noise map) which are then used to estimate the peak brightness and finally compared with that of our real map². The result for the circular gaussian is shown

²Due to possible imperfect correlation on the longest baselines, a 10% loss in the measurement of the peak brightness is also accounted for

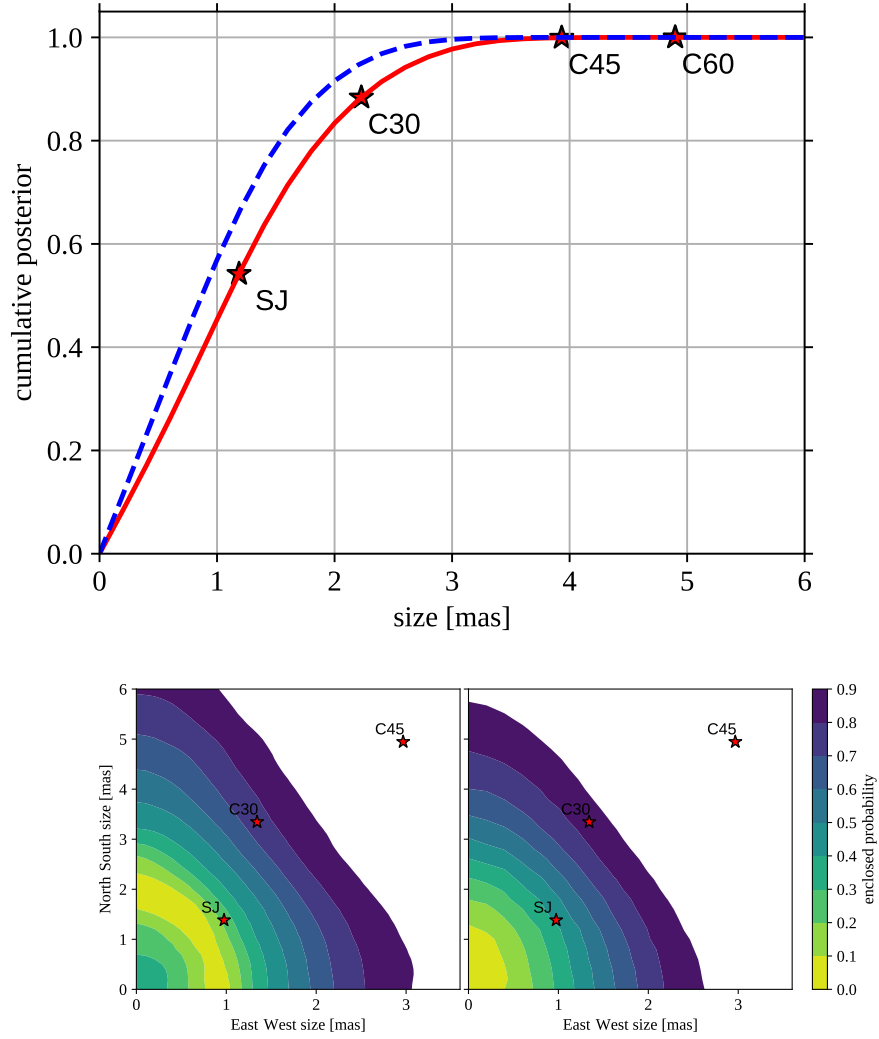


Figure 3: Size constraints. Top panel: Bayesian posterior probability on the source size (for the circular Gaussian case) assuming a flat prior for the total brightness and requiring that, for each source size the peak brightness is consistent with the measured value ($42 \pm 8 \mu\text{Jy/beam}$). The blue dashed line accounts for the possible 10% losses due to imperfect correlation. Bottom panel: same as for the top panel but for the two dimensional Gaussian model for the source size. The two models discussed in this manuscript are the SJ=structured jet and C30=cocoon model with 30 degrees of aperture.

in Fig.3 (top panel). This shows that the source size is < 2.5 mas at the 90% confidence level and argues against the asymmetric cocoon model (C30) which is marginally consistent with such a constrain. The same holds for the two dimensional constraints (shown in the bottom panels of Fig.3).

3. Conclusions

The global EVN observation at 5 GHz of the electromagnetic counterpart of GRB/GW170817

204,7 days after the discovery, caught the source near the peak of its light curve with a detected peak brightness of $42 \pm 8 \mu\text{Jy}/\text{beam}$. The source appear compact and unresolved in our image and we estimate (Fig.3) an upper limit of 2.5 mas on the source size (at the 90% confidence level). This argues against the cocoon scenario which should be more extended and thus resolved in our image (Fig.2). Instead a gaussian structured jet with a core opening angle of 3.4° with an isotropic kinetic energy of $\sim 2.5 \times 10^{52}$ erg seen under a viewing angle³ of 15° is consistent with our size measurement. A Gaussian structured jet with similar parameters is also inferred from the interpretation of the measurement of the source proper motion along the three epochs (75 and 230 days - [10] - and 204 days - [27]).

The presence of structured jet has two primary consequences: it tells us that the merger of the two neutron stars producing the GW signal is also responsible for the launch of a jet that successfully breaks out of the merger material that is torn apart by the merger itself and which is responsible for the kilonova emission. According to the recent estimates of the luminosity function of short GRBs [31, 32], the rate of high luminosity short GRBs (with $L_{\text{iso}} > 10^{51}$ erg/s) is $\sim 0.5 \text{ yr}^{-1} \text{ Gpc}^{-3}$. If we assume a structured universal jet, adopting the formalism of Pescalli et al. (2015), the rate of short GRBs with lower luminosity increases reaching a rate of events with $L_{\text{iso}} > 10^{47}$ erg/s (i.e. GRB170817) of $\sim 200\text{--}600 \text{ yr}^{-1} \text{ Gpc}^{-3}$ (according to the specific jet energy structure adopted - see Fig.4 of [27]). With respect to the rate of GW events as derived from GW170817 [2], our results suggest that up to 10% of binary mergers can produce a successful jet (successful in breaking out of the merger ejecta which probably play a relevant role in shaping the jet structure). The detection of new events in the forthcoming LIGO/VIRGO observational run will probe these scenarios in more details.

Acknowledgements. Funding from the European Union’s Horizon 2020 research and innovation programme under grant agreement No 730562 [RadioNet] is acknowledged. I am grateful to the complete list of authors that allowed to perform such a challenging observation, analyse the data and interpret them. M. Orienti is acknowledged for useful discussion and fast scrutiny of some data of this observational campaign. Acknowledgements

References

- [1] Abbott, B., et al. 2016a, Phys. Rev. Lett., 116, 061102
- [2] Abbott, B., et al. 2017, ApJ, 848, L13
- [3] Goldstein, A., et al. 2017, ApJ, 848, L14
- [4] Zhang, B. B., et al., 2018, Nat. Comm., 9, 447
- [5] Savchenko, V., et al., 2017, ApJ, 848, L15
- [6] D’Avanzo, P., et al., 2014, MNRAS, 442, 2342
- [7] Valenti, S., et al., 2017, ApJ, 848, L24
- [8] Coulter, D. A., et al., 2017, Science , 358, 1556

³The viewing angle we infer is consistent with the inclination angle of 151_{-11}^{+15} deg derived from the modelling of the GW signal (Abbott et al. 2018).

- [9] Pian, E., et al., 2017, *Nature*, 551, 67
- [10] Mooley, K. P., et al., 2018, *Nature*, 2018, 554, 207
- [11] Mooley, K. P., et al., 2018a, *Nature*, 2018, 561, 355
- [12] Mooley, K. P., et al., 2018b, *ApJ*, 868, 11
- [13] Troja, E., et al., 2017, *Nature*, 551, 71
- [14] Margutti, R., et al., 2017, *ApJ*, 848, L20
- [15] Lyman, J. D., et al., 2018, *Nat. Astr.*, 2, 751
- [16] D’Avanzo, P., et al., 2018, *A&A*, 613, L1
- [17] Perego, A., Radice, D., Bernuzzi, S., *ApJ*, 850, L37
- [18] Arcavi, I., et al., *Nature*, 551, 64
- [19] Salafia, O. S., Ghisellini G., Ghirlanda G., 2018, *MNRAS*, 474, L7
- [20] Hallinan, G., et al., 2017, *Science*, 358, 1579
- [21] Alexander, K. D., et al., 2017, *ApJ*, 848, L21
- [22] Haggard, D., et al., 2017, *ApJ*, 848, L25
- [23] Gottlieb, O., Nakar, E., Piran, T., 2018, *MNRAS*, 473, 576
- [24] Nakar, E. & Piran, T., 2017, *ApJ*, 834, 28
- [25] Lazzati, D., et al., 2018, *PhRvL*, 120, 1103
- [26] Resmi, L., et al., 2018, *ApJ*, 867, 57
- [27] Ghirlanda, G., et al., 2018, arXiv:1808.00469
- [28] Gill, R., & Granot, J., 2018, *MNRAS*, 478, 4128
- [29] Zrake, J., Xie, X., MacFadyen, A., 2018, *ApJ*, 856, L2
- [30] Corsi, A., et al., 2018, *ApJ*, 861, L10
- [31] Wanderman, D., Piran, T., 2015, *MNRAS*, 448, 3026
- [32] Ghirlanda, G., et al., 2016, *A&A*, 594, 84